Arabian Journal of Chemistry (2019) 12, 946–956

King Saud University

Arabian Journal of Chemistry

www.ksu.edu.sa
www.sciencedirect.com

ORIGINAL ARTICLE

An enhanced electrocatalytic oxidation and determination of 2,4-dichlorophenol on multilayer deposited functionalized multi-walled carbon nanotube/Nafion composite film electrode

Noha Al-Qasmi [a,b], M. Tahir Soomro [a,*], Iqbal M.I. Ismail [a,b], Ekram Y. Danish [b], Attieh A. Al-Ghamdi [c]

[a] *Center of Excellence in Environmental Studies, King Abdulaziz University, P.O. Box 80216, Jeddah 21589, Saudi Arabia*
[b] *Chemistry Department, Faculty of Science, King Abdulaziz University, P.O. Box 80216, Jeddah 21589, Saudi Arabia*
[c] *Center of Nanotechnology, King Abdulaziz University, Jeddah, P.O. Box 80216, Jeddah 21589, Saudi Arabia*

Received 29 June 2015; accepted 29 August 2015
Available online 8 September 2015

KEYWORDS

2,4-Dichlorophenol;
Electrocatalytic oxidation;
Multi-walled carbon nanotube/Nafion composite;
Electrochemical sensor;
Voltammetry

Abstract The voltammetric (CV and DPV) behavior of multi-walled carbon nanotube/Nafion composite coupled with a glassy carbon electrode was investigated for the determination of 2,4-dichlorophenol. The structural and morphological evaluation by XRD and FESEM revealed that the acid treated MWCNT retained their morphology without any structural change. The existence of the possible functional groups was investigated by FTIR and Raman spectroscopy. Compared to bare GCE, a significantly reduced interfacial charge transfer resistance was noticed for MWCNT/Nafion/GCE by electrochemical impedance spectroscopy (EIS). The use of Nafion not only contributed to the non-covalent functionalization of MWCNT, but also protected the electrode surface against the polymerization of phenoxy radicals forming a passivating film. For MWCNT/Nafion/GCE, the combination of anti-passivating ability and excellent catalytic properties resulted in the rapid and direct electrochemical determination of 2,4-DCP. Under optimal experimental

* Corresponding author.
E-mail addresses: soomro.m.tahir@gmail.com, msoomro@kau.edu.sa (M. Tahir Soomro).
Peer review under responsibility of King Saud University.

Production and hosting by Elsevier

http://dx.doi.org/10.1016/j.arabjc.2015.08.032

conditions, the DPV responses for MWCNT/Nafion/GCE is linear over the 1–150 μmol/L range with a detection limit (S/N = 3) of 0.01 μmol/L. The presence of many interfering species had no influence on the signals of 2,4-DCP. The proposed sensor was successfully tested for the determination of 2,4-DCP in tap water samples and the recovery was in the range of 99.0–102.5%.

1. Introduction

The presence of toxic organic pollutants is ubiquitous in domestic and industrial effluent. Over the last few decades, there has been a growing interest regarding the detection and removal of these chemicals (Aslam et al., 2014, 2015a,b, 2016; Bashami et al., 2015; Tasic et al., 2014; Yu et al., 2015). 2,4-Dichlorophenol (2,4-DCP) regarded as priority pollutant is a highly carcinogenic and acutely/chronically toxic compound to humans (Jantra et al., 2005; Sherly et al., 2014). The major sources of release of this compound in the environment are likely to be the production of 2,4-DCP and its use as intermediates in the production of higher chlorinated phenols and other key compounds (Ureta-Zañartu et al., 2002; Pirvu et al., 2010; Ho et al., 2012). The chemical stability as well as resistance to biodegradation of 2,4-DCP, the detection of 2,4-DCP becomes one of the important tasks for public safety. Therefore, it is of great significance to develop a simple, sensitive, and reliable analytical approach for the rapid and direct detection of 2,4-DCP.

Although the instrumental methods including gas–liquid or liquid chromatography and optical spectroscopy offer high sensitivity for determination of, 2,4-DCP, the associated disadvantages in terms of cost, complexity, time consumption, and lack of portability are unavoidable (Tong et al., 2013; Li et al., 2013; Fan et al., 2015a,b; Kolliopoulos et al., 2015; Lu et al., 2015; Feng et al., 2011; Li et al., 2008a; Wei et al., 2015). In recent years, electrochemical methods have become an alternative to conventional instrumental methods for direct determination of 2,4-DCP due to their compatibility for on-site measurements (Zhang et al., 2013a; Sun and Zhang, 2006; Arribas et al., 2011; Safavi et al., 2014; Ozsoz et al., 2003; Tonle et al., 2015; Ozkan et al., 2002; Shi et al., 2015; Wang et al., 2000; Xu et al., 2012; Yang et al., 2012). These methods are inexpensive, fast, and simple in operation. Electrochemical detections based on pulse techniques showed great promise because of their high sensitivity, superior efficiency, and low detection profile (Amin et al., 2014; Chen and Shah, 2013) and therefore, can be used for vast analyte spectrum.

When 2,4-DCP is oxidized at positive potentials, the phenoxy radicals produced can undergo polymerization reaction resulting in the formation of polymeric adherent film on the electrode surface. This poisoning of the electrode surface due to passivating films prevents electron transfer processes at

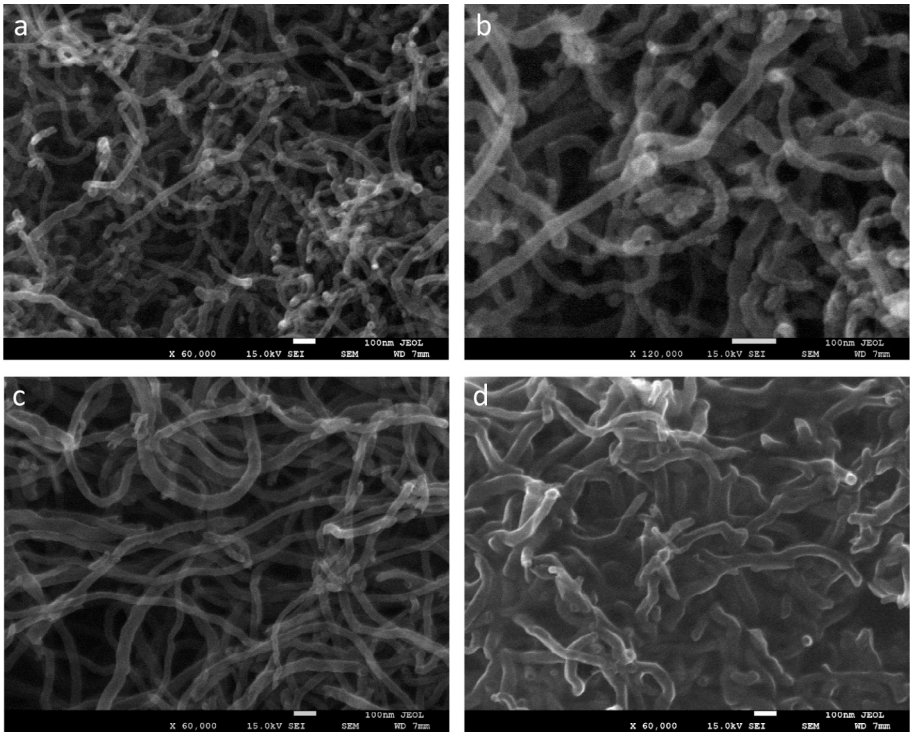

Figure 1 FESEM images of MWCNT at (a) 60,000× (b) 120,000 while (c) and (d) are the FESEM images of acid treated MWCNT and MWCNT/Nafion composite film at 60,000×.

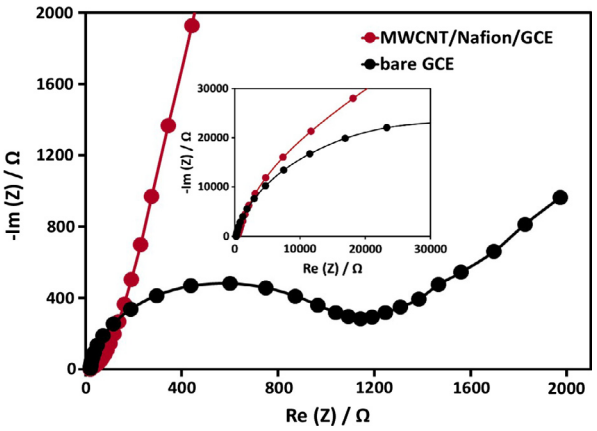

Figure 2 EIS Nyquist plot of bare GCE and MWCNT/Nafion/GCE in 2 mmol/L $[Fe(CN)_6]^{3-}$ and 0.1 mol/L pH 6.0 phosphate buffer. The inset shows the Nyquist plot of the EIS of bare GCE and MWCNT/Nafion/GCE in 100 μmol/L 2,4-DCP and 0.1 mol/L pH 6.0 phosphate buffer.

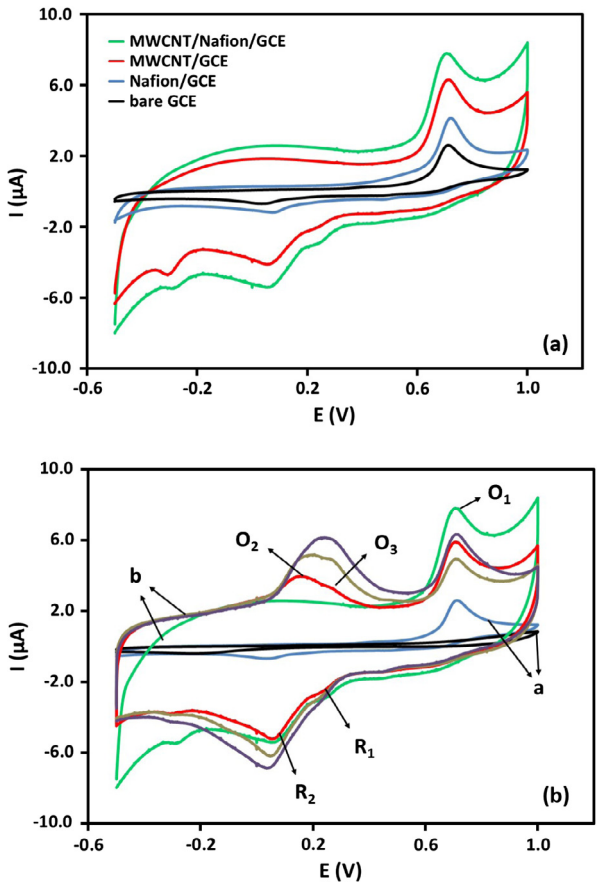

Figure 3 (a) The CV comparison of bare GCE, Nafion/GCE, MWCNT/GCE, and MWCNT/Nafion/GCE in 0.1 mol/L pH 6.0 phosphate buffer containing 100 μmol/L of 2,4-DCP. (b) Multi-CV scans of bare GCE (curves a, first and last scan) and MWCNT/Nafion/GCE (curves b, first, second, fifth and tenth scans, respectively).

the electrode/electrolyte interface and therefore, no further oxidation of 2,4-DCP is possible (Safavi et al., 2014; Ureta-Zañartu et al., 2001; Ezerskis and Jusys, 2001; Ežerskis and Jusys, 2001; Biniak et al., 2015). Studies have shown that the prevention of electrode passivation is still a challenge, which can be achieved by using the new electrode material (Biniak et al., 2015). Since their discovery, the multi-walled carbon nanotubes have been demonstrated to be a very efficient sensing material, especially for electroanalytical detection (Wang et al., 2003; Pontié et al., 2011; Lü et al., 2013; Barsan et al., 2015; Li et al., 2008b; Trojanowicz, 2006) due to their high specific surface area, excellent catalytic activity, adsorption capability, superior electric and mechanical properties (Barsan et al., 2015; Li et al., 2008b; Trojanowicz, 2006). Moreover, functionalization of multi-walled carbon nanotubes imparts higher solubility and processability, enabling their use as catalytically active material for electrochemical applications. Nafion is a perfluorinated cation exchange membrane with ideal properties of electrochemical inactivity, chemical stability, anti-passivating properties and owing to its hydrophilicity, a well-dispersed MWCNT/Nafion composite can be prepared (Yang et al., 2010; Lee et al., 2011; Ijeri et al., 2010; Zhang et al., 2013b). This functionalized composite can be easily coated on a glassy carbon electrode (GCE) surface to prepare MWCNT/Nafion/GCE. To the best of our knowledge, the proposed electrochemical method is promising for on-site detecting of 2,4-DCP residue due to its better detection limit.

This study demonstrated that MWCNT/Nafion composite coupled with a glassy carbon electrode had an excellent electrocatalytic activity toward oxidation of 2,4-DCP. Well-shaped and remarkably improved oxidation peak for 2,4-DCP was due to porosity, the increase of the superficial area of modified electrode, and diffusion of 2,4-DCP molecules from the surface to the inner layers of the modified electrode. The exhibited higher catalytic activity, reproducibility, and sensitivity of functionalized MWCNT are attributed to the synergic effect, the composite of MWCNT and Nafion.

2. Experimental

2.1. Reagents and solutions

All the solutions were prepared in deionized water from a Milli-Q® Gradient water purification system (Millipore SAS, Molsheim, France). The stock solution (1 mmol/L) of 2,4-DCP (Sigma Aldrich, 99%) was prepared with 0.1 mol/L pH 6.0 phosphate buffer. The test solutions of desired concentrations were prepared on day-to-day by diluting the stock solution by phosphate buffer. Phosphate buffer in the pH range of 4–8 was prepared by mixing the appropriate amount of 0.5 mol/L NaOH and 0.5 mol/L H_3PO_4. The 1% solution of Nafion® perfluorinated resin was prepared by diluting the 5% solution (Sigma Aldrich) in deionized water. MWCNT with average diameters of 20–50 nm was purchased from Adneno Technologies, India.

2.2. Preparation of MWCNT/Nafion composite film electrode

The MWCNT/Nafion composite film was casted by a simple drop coating method onto the surface of the polished glassy

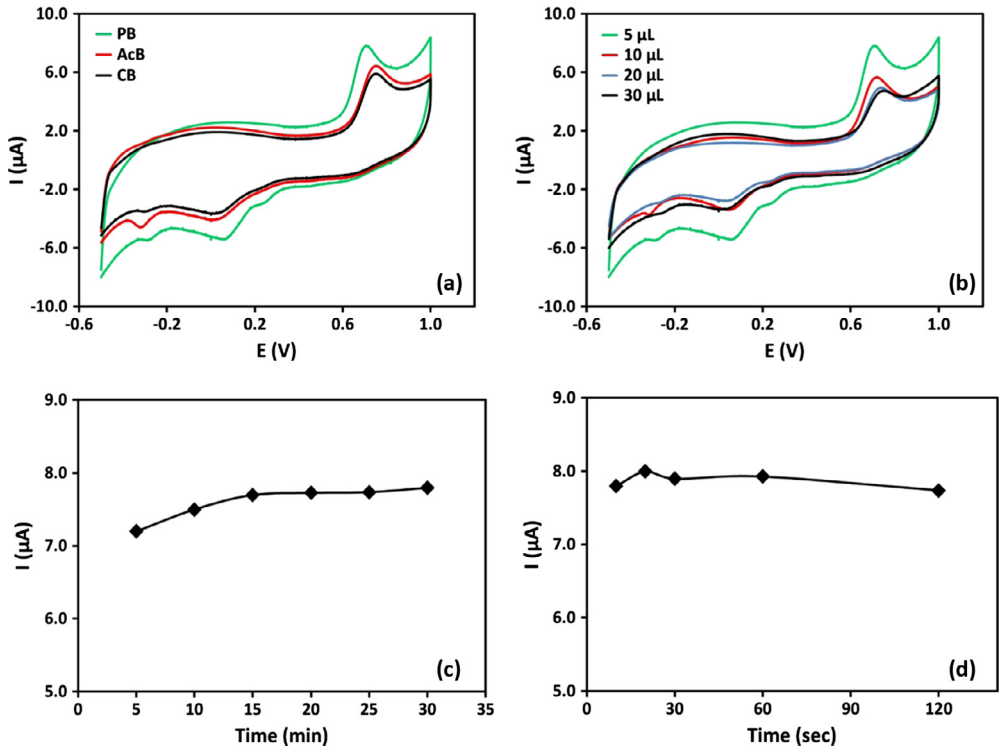

Figure 4 (a) CVs of MWCNT/Nafion/GCE in 0.1 mol/L pH 6.0 phosphate buffer, acetate buffer, and citrate buffer containing 100 μmol/L of 2,4-DCP. (b) CVs of MWCNT/Nafion/GCE with different film thickness of MWCNT/Nafion composite. (c) Effect of N_2 gas purging. (d) Effect of stirring.

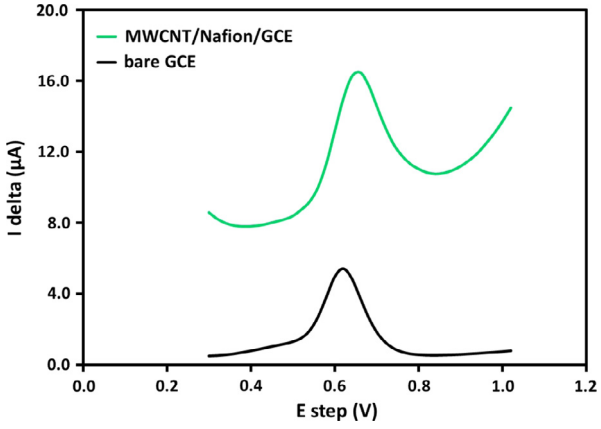

Figure 5 DPV curves of bare GCE and MWCNT/Nafion/GCE in 0.1 mol/L pH 6.0 phosphate buffer containing 100 μmol/L 2,4-DCP.

carbon electrode (GCE). Prior to composite formation, MWCNT with high porosity and open end hydrophilic surfaces was obtained by boiling in concentrated HNO_3 for 4 h followed by rinsing with deionized water. The MWCNT/Nafion composite was prepared by dispersing 0.5 mg of MWCNT in 1 mL of 1% Nafion solution under sonication. For preparation of MWCNT/Nafion/GCE, 5 μL of MWCNT/Nafion composite was dripped onto the tip of the GCE and allowed to dry under N_2. The uniformity of the MWCNT/Nafion composite film coated on GCE was examined optically.

2.3. Instrumentation

Electrochemical measurements were performed with a VSP multi-channel potentiostat (Bio-logic Science, USA) equipped with ECLab software for data analysis. The MWCNT/Nafion composite supported on glassy carbon electrode (electrode size, OD = 6 mm, ID = 3 mm) was used as working electrode whereas Ag/AgCl/saturated KCl and platinum wire were used reference and auxiliary electrodes, respectively. All the measurements were performed at 25 °C. The electrochemical impedance spectroscopic (EIS) measurements were recorded at open circuit voltage (OCV) in 0.1 mol/L pH 6.0 phosphate buffer containing 100 μmol/L 2,4-DCP, and at a biased potential of +0.233 V in 0.1 mol/L KCl containing 2 mmol/L $[Fe(CN)_6]^{3-}$. The EIS frequencies were scanned from 10^5 Hz down to 1 Hz, whereas analysis of EIS data was carried out using Z-fit (ECLab Software). The FT-IR spectra were acquired in the range of 400–4000 cm^{-1} using a Shimadzu IRAffinity-1. The XRD pattern was recorded by Ultima-IV X-ray diffractometer (Rigaku, Tokyo, Japan) equipped with a Cu $K\alpha$ radiation source. The surface analysis of the MWCNT and MWCNT/Nafion composite was performed by field emission scanning electron microscope (FESEM) JEOL (Tokyo, Japan) JSM 7600F on a silicon wafer substrate. Raman shifts were measured by using a DXR Raman Microscope (Thermo Scientific, USA) using a 532 nm laser as the excitation source at 6 mW power.

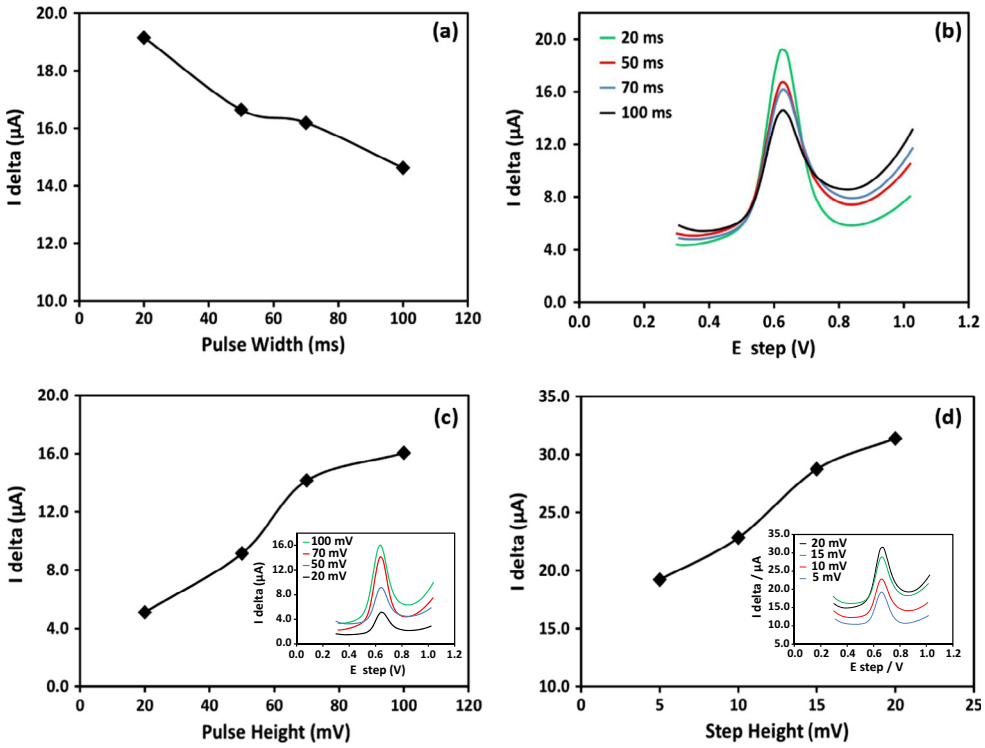

Figure 6 (a) Effect of varying pulse width on oxidation current. (b) Corresponding DPV curves. (c) Effect of varying pulse amplitude on oxidation current with corresponding DPV curves in the inset. (d) Effect of varying step potential on oxidation current with corresponding DPV curves in the inset.

2.4. Electrochemical detection

For electrochemical analysis, a 10 mL solution of 0.1 mol/L pH 6.0 phosphate buffer containing 100 µmol/L of 2,4-DCP was introduced into the electrochemical cell. Before measurements, the test solution was purged with N_2 gas for the removal of dissolved oxygen. The CV behavior was recorded by sweeping the potential between −0.5 V and +1.0 V with a scan rate of 100 mV/s. DPV with initial potential (E_{in}) = +0.2 V, final potential (E_{fin}) = +1.0 V, equilibrium time of 10 s, pulse width of 50 ms, pulse height of 50 mV, scan rate of 20 mV/s was employed. Blank measurements were performed in 0.1 mol/L pH 6.0 phosphate buffer.

2.5. Preparation and analysis of tap water samples

The tap water samples collected from Jeddah, Saudi Arabia, were stored at 4 °C. Before analysis, the samples were filtered with a 0.45 µm membrane filter, and transferred into volumetric flasks that were filled with deionized water. For electrochemical measurements a required amount of tap water samples was diluted with 0.1 mol/L pH 6.0 phosphate buffer up to 10 mL. After deaeration with N_2 gas, the DPV signals were registered under optimal conditions.

3. Results and discussion

3.1. Spectral characterization of functionalized MWCNT

The structural investigation of MWCNT, performed by X-ray diffraction analysis is shown in Supplementary Fig. S1. In the XRD pattern, an intense reflection at $2\theta = 26.1°$ and a weak reflection at $2\theta = 42.8°$ arising from the (002) and (100) face were in good agreement with the previous literature values (Zhang et al., 2011; Chen and Oh, 2011; Berhanu et al., 2009). Being the measure of the crystallinity and crystallite size, the intensity of the reflection at $2\theta = 26.1°$ depicted the highly crystalline nature and large crystallite size. No significant change in the XRD pattern due to the acid treatment of MWCNT was apparent that elaborated the suitability of the purification process without any significant damage to crystalline structure of MWCNT.

Raman spectroscopic analysis is regarded as an appropriate tool for the recognition of sp^2 hybridized carbon systems as well as the local defects in the MWCNT (Datsyuk et al., 2008; Stancu et al., 2011). As presented in Supplementary Fig. S2, two distinct bands are evident in the Raman spectra of MWCNT, before and after acid treatment. The G-band at 1570 cm^{-1} represents the sp^2 carbon system, whereas D-band at 1330 cm^{-1} reflects the disordered carbons in the MWCNT structure. The appearance of the mirror image after acid treatment revealed no significant effects occurred to the lattice of MWCNT. However, the decrease intensity of D-band and the slight increase in the intensity of G-band signified the likely removal of amorphous carbon impurities and metal particles from the surface of the MWCNT (Stancu et al., 2011). The relative intensity ratio of D/G bands (I_D/I_G) is a measure of the purity and the defect density of MWCNT (Grassi et al., 2012). In the current case, the estimated ratio of 1.059 for untreated MWCNT and 0.90 for acid treated MWCNT depicted the decreased extent of defects in purified MWCNT.

The typical FTIR spectra of as received and acid treated MWCNT are presented in Supplementary Fig. S3. As can be

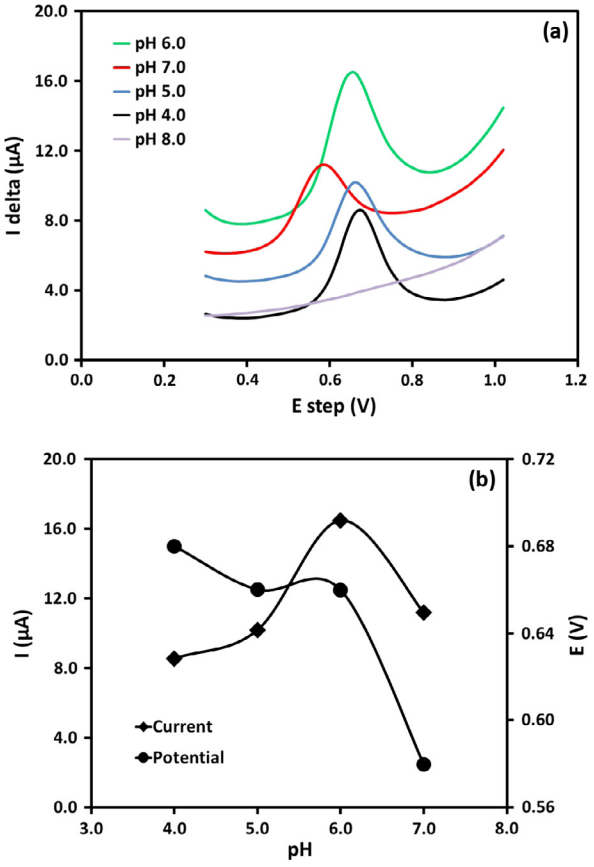

Figure 7 (a) pH dependent DPV curves of MWCNT/Nafion/GCE in 0.1 mol/L pH 6.0 phosphate buffer containing 100 µmol/L 2,4-DCP. (b) Variation of oxidation peak current and oxidation peak potential with pH.

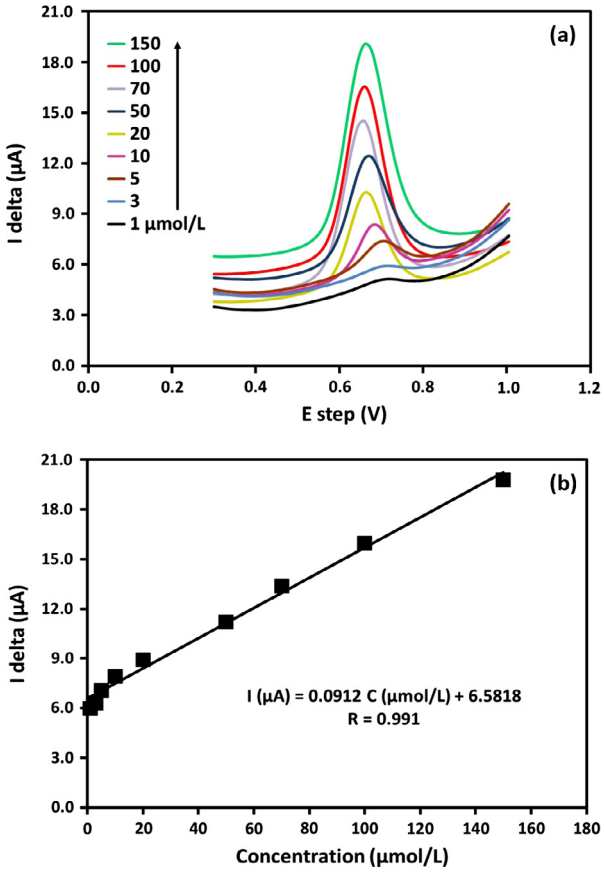

Figure 8 (a) DPV curves of MWCNT/Nafion/GCE with different concentrations of 2,4-DCP. (b) Corresponding calibration plot.

seen, there is not much difference in the intensities of the stretching vibrations of carbonyl, carboxyl, and hydroxyl groups at 1655 cm^{-1}, 1721 cm^{-1}, and 3440 cm^{-1} before and after acid treatment process, which indicates that the boiling of MWCNT in concentrated nitric acid for 4 h led to the removal of the impurities with least detrimental effect on the lattice of MWCNT. Apart from this observation, no additional information was extractable from the spectrum of acid treated MWCNT in comparison with that of untreated. Additionally the sharp peak observed at 2368 cm^{-1} in both represented the CO_2 coating of IR optics (Saleh, 2013; Gupta and Saleh, 2001).

The FESEM images of as received MWCNT at 60,000× and 120,000× are shown in Fig. 1a and b whereas that of acid treated and MWCNT/Nafion composite film are presented in Fig. 1c and d. The comparison of the FESEM images revealed no obvious change in the morphology of the MWCNT after acid purification process. The MWCNT retained its fibrous structure without any significant variation. The FESEM results were in complete agreement with XRD, Raman and FT-IR results. Moreover, the FESEM image of MWCNT/Nafion composite as presented in Fig. 1d implied that the dispersion of MWCNT leads to the formation of a homogeneous multilayer film without any apparent irregularities.

3.2. Impedance measurement

The electrochemical impedance spectroscopy (EIS) is an effective approach for correlating the charge transfer resistance and electrocatalytic activity of the electrode as a result of the surface modification (Bashami et al., 2015; Amin et al., 2014; Zheng et al., 2012). The comparison of the resulting EIS Nyquist plot of bare GCE and MWCNT/Nafion/GCE in 2 mmol/L $[Fe(CN)_6]^{3-}$ solution is shown in Fig. 2. The absence of the semicircle for MWCNT/Nafion/GCE at high frequency, in comparison with that of bare GCE, depicted an enhanced ionic conductivity at the electrode–electrolyte interface. It is obvious that the lowest charge transfer resistance of MWCNT/Nafion/GCE would result in improving the catalytic activity of the modified electrode and facilitate the highly sensitive detection of 2,4-DCP. The EIS Nyquist behavior of bare GCE and MWCNT/Nafion/GCE was evaluated in 100 µmol/L 2,4-DCP and 0.1 mol/L pH 6.0 phosphate buffer are presented in the inset of Fig. 2. The MWCNT/Nafion/GCE possessed low resistance of the charge transfer and, therefore, better analytical detection. The result is in accordance with the EIS analysis of MWCNT/Nafion/GCE in $[Fe(CN)_6]^{3-}$.

Table 1 Comparison of the analytical performance of the proposed method with some reported methods.

Detection methods	LOD[a] (μmol/L)	DLR[b] (μmol/L)	*R*	Ref.
DPV	0.01	1–150	0.991	This work
DPV	1.6	5–100	0.9951	Zhang et al. (2013)
FIA	0.037	0.1–100	0.9997	Arribas et al. (2011)
Chemiluminescence	0.085	0.614–122.7	0.9990	Feng et al. (2011)
Amperometry	0.38	1–100	0.9995	Barsan et al. (2015)
Amperometry	20	10–300	0.9937	Pirvu et al. (2010)
UV–Vis	0.23	1–9.0	0.976	Tong et al. (2013)
HPLC	0.001	0.0092–1.84	0.9995	Li et al. (2013)
HPLC	0.0047	0.3–12.3	0.9999	Feng et al. (2009)
GC/MS	0.00008	0.0006–6	0.9990	Ho et al. (2012)

[a] Limit of detection.
[B] Dynamic linear range.

Table 2 Interferences of some organic and inorganic compounds on the determination of 2,4-DCP.

Interferences	Tolerance level (μmol/L)	RSD (%)
2-CP, 3-CP, 4-CP	20	5.1
2-NP, 3-NP, 4-NP, 2,4-DNP	400	3.4
Zn^{2+}, Cu^{2+}, Co^{2+}, Pb^{2+}, SO_4^{2-}	500	2.2
NH_4^+, Na^+, K^+, Cl^-	500	2.2

3.3. Electrochemical behavior of 2,4-DCP at MWCNT/Nafion/GCE

The electrochemical behavior of bare and modified GCE electrodes (Nafion/GCE, MWCNT/GCE, and MWCNT/Nafion/GCE) by sweeping the cyclic voltammetric (CV) potential between −0.5 V and +1.0 V in 0.1 mol/L pH 6.0 phosphate buffer containing 100 μmol/L 2,4-DCP at a scan rate of 50 mV/s was studied. The typical CV curves were recorded are shown in Fig. 3a. As can be seen, at bare GCE the oxidation and reduction peaks associated with 2,4-DCP were weak. However, upon sweeping the same potential window with Nafion/GCE, MWCNT/GCE, and particularly with MWCNT/Nafion/GCE the gradual increase in the redox peak currents was observed. The CV results mean that the MWCNT/Nafion composite had higher electrocatalytic activity than both MWCNT and Nafion. The high porosity and non-covalent functionalization of sulfonate contents on the surface of MWCNT by integration of Nafion would enable the formation of multilayer film on the surface of GCE. Thus, the synergic effect of MWCNT and Nafion as a co-catalyst

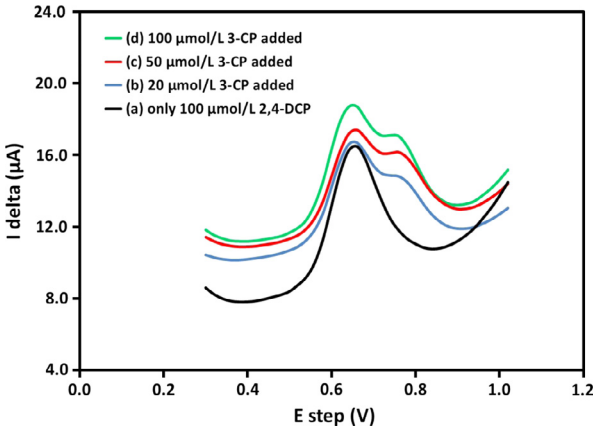

Figure 9 DPV curves of MWCNT/Nafion/GCE in (a) 100 μmol/L 2,4-DCP only and (b–d) 100 μmol/L 2,4-DCP with 20, 50, and 100 μmol/L 3-CP.

with highly improved electrocatalytic activity made MWCNT/Nafion a good electrode material for the sensitive detection of 2,4-DCP.

The electrochemical behavior of 2,4-DCP at MWCNT/Nafion/GCE was analyzed. The first scan of MWCNT/Nafion/GCE showed a well-defined irreversible oxidation peak "O_1" for 2,4-DCP at ~+0.70 V, and two weak reduction peaks "R_1", "R_2" at ~+0.23 V and ~+0.06 V, respectively. Related to R_1 and R_2, their corresponding oxidation peaks "O_2" and "O_3" unveiled during the second scan of multi-CV analysis of MWCNT/Nafion/GCE (Fig. 3b) at ~+0.15 V and ~+0.26 V. However, with the increase in the number of scans, the two weak redox peak pairs (O_2/R_2 and O_3/R_1) were combined and appeared as a single redox pair rather than two. Here, based on experimental evidences, it is interpreted that the origin of these quasi-reversible CV redox pairs (O_2/R_2 and O_3/R_1) is the formation of soluble quinone-like products.

The passivation of bare and modified GCE, typically related to the oxidation of 2,4-DCP, was estimated by performing multi-CV analysis. The comparison of the multi-CV scans of bare GCE (curves a) and of MWCNT/Nafion/GCE (curves b) is presented in Fig. 3b. The oxidation peak "O_1" as well as barely detected reduction peak revealed during the first CV scan at bare GCE were gradually decreased in their intensities to the point where no peak appeared at all that depicted the complete coverage of the electrode surface by the polymeric passivating film and resulted in the loss of electrode activity. Such type of deactivation of the electrode surface was not observable with MWCNT/Nafion/GCE that reflected the resistance of the MWCNT/Nafion composite layer against electrode passivation. The stable and reproducible response with MWCNT/Nafion/GCE in multi-CV analysis, from the first scan to tenth scan, was attributed to the porous structure of MWCNT and proton exchange properties of Nafion that supported the free passage of 2,4-DCP molecules from the outer surface of the electrode to the inner layers.

3.4. Experimental conditions

Since the sensitivity of the proposed method is based on the electrochemical signal, the 2,4-DCP measurements related

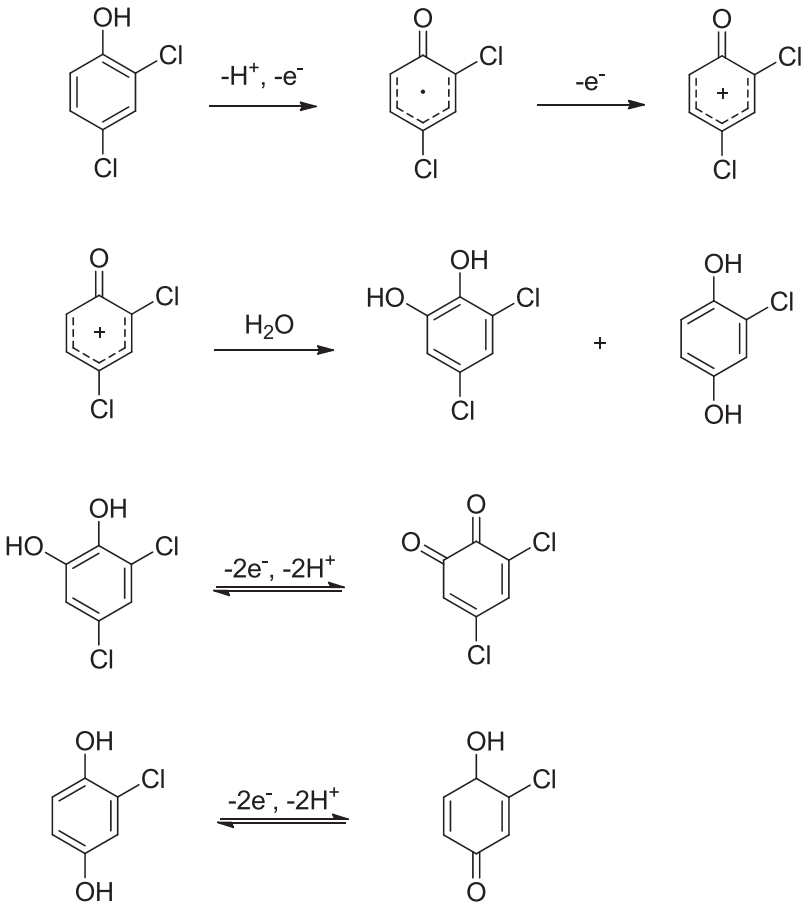

Scheme 1 Possible electrochemical reaction mechanism of oxidation of 2,4-DCP at MWCNT/Nafion/GCE.

Table 3 Determination results of 2,4-DCP in tap water samples.

Added (μmol/L)	Found (μmol/L)	Recovery (%)	RSD (%)
20	19.8	99.0	2.3
50	51.25	102.5	1.9
70	69.86	99.8	2.0

factors were optimized. Fig. 4a shows the comparison of the CV behavior of 2,4-DCP at MWCNT/Nafion/GCE evaluated in different electrolytes such as phosphate buffer (PB), acetate buffer (AcB), and citrate buffer (CB). Although the CV pattern of 2,4-DCP in all the three electrolytes is identical, an enhanced and well-resolved oxidation peak "O_1" was recognized in phosphate buffer. More importantly, the low overpotential for oxidation of 2,4-DCP realized in phosphate buffer obviously in favor of its selection as an optimal electrolyte, therefore, subsequent measurements were carried out in phosphate buffer.

The variation in the CV behavior of 2,4-DCP with the changing density of MWCNT/Nafion composite layer on GCE surface is shown in Fig. 4b. It was inferred that by increasing the thickness of MWCNT/Nafion composite film, the oxidation as well as the reduction peak currents gradually decreases in addition to a positive shift in oxidation peak "O_1". Pure MWCNT being porous and hydrophobic in nature (Govindhan et al., 2015), forms a loose and porous film on GCE due to poor dispersity. The same is evident from the FESEM images. The application of Nafion as a co-modifier with MWCNT, besides the preconcentration of 2,4-DCP molecules at the modified electrode surface, helps to eliminate the lackness of the film that results in highly conductive and porous multi-layer film of MWCNT/Nafion composite. The pores support the diffusion of 2,4-DCP molecules from the surface of the electrode to the inner layers of the modified electrode, however, with the increased density of MWCNT/Nafion composite the porosity of the film is decreased, which retards the electron transfer and mass transportation of 2,4-DCP. Based on the measurement with the films of varying thickness, a 5 μL of 0.5 mg/ml MWCNT/Nafion suspension was recognized as the optimal volume for the preparation of MWCNT/Nafion/GCE.

The diffusion behavior of 2,4-DCP at MWCNT/Nafion/GCE was researched. The N_2 gas was purged for 5–30 min with the interval of 5 min between two repeated measurements. The variation in oxidation peak current of 2,4-DCP versus N_2 gas purging time is shown in Fig. 4c whereas in Fig. 4d the oxidation current of 2,4-DCP measured in a continuous stirred solution with different time intervals, is presented. No obvious change occurred in the oxidation current, therefore, the determination of 2,4-DCP is purely a diffusion controlled process that can be performed in quiescent solution without nitrogen purging.

3.5. DPV detection of 2,4-DCP

Under optimized experimental conditions, differential pulse voltammetric (DPV) responses of 2,4-DCP at bare GCE and MWCNT/Nafion/GCE are shown in Fig. 5. As expected, 2,4-DCP yields a significantly enhanced oxidation peak at MWCNT/Nafion/GCE (at ~+0.70 V) compared with that of bare GCE. The effects of initial potential, pulse width, pulse amplitude, and scan rate on the detection of 2,4-DCP were optimized. The initial potential was in the range of −0.3 V to +0.3 V afforded a better reproducible peak with E_{in} = +0.3 V. The variation in oxidation peak current with a variable pulse width from 20 ms to 120 ms is depicted in Fig. 6a and b. A linear decrease in the peak current with increasing the pulse width was observed. The optimum pulse amplitude was obtained by varying the pulse amplitude from 20 to 120 mV (Fig. 6c). Conversely, with respect to pulse width, the peak current increased linearly with the increase of pulse amplitude, however, above 100 mV slight broadening of the peak was noticed. The step height or pulse increment was examined in the range of 5–25 mV (Fig. 6d). The peak current increased linearly with the increasing pulse increment. At an increment higher than 20 mV, the peak shape lost its feature, sharpness, and smoothness. Similar to variations in pulse amplitude and pulse increment, an increase in pulse width greater than 100 ms resulted in the broadness of peak shape. To summarize the optimization of parameters, the optimum DPV signal for 2,4-DCP was witnessed at a pulse width of 50 ms, pulse amplitude of 50 mV, and pulse increment of 10 mV (or scan rate of 20 mV/s). Therefore, the subsequent DPV measurements were at the optimized parameters mentioned above.

The DPV coupled with anodic stripping step was performed in 100 µmol/L 2,4-DCP and 0.1 mol/L pH 6.0 phosphate buffer. The DPV signals at an accumulation potential of +0.2 V as well as under open circuit potential with an accumulation time ranging from 0 to 60 s showed almost no influence on the oxidation peak current and the peak potential of 2,4-DCP. The oxidation peak shape more or less remained unchanged. This observation led to the inference that the detection of 2,4-DCP can be realized without stripping mode.

3.6. pH study and reaction mechanism of 2,4-DCP

The pH of the electrolyte is an essential parameter and greatly affects the oxidation mechanism of 2,4-DCP. To evaluate the effect of pH using MWCNT/Nafion/GCE, the DPV analysis in a pH range of 4.0–8.0 was explored (Fig. 7a). The variation in the oxidation peak current and oxidation peak potential as a function of pH is presented in Fig. 7b. An increase in the peak current was noted with the increase of the pH till 6.0 followed by a sharp decrease whereas the shift in the peak potential toward less positive potential signifies the participation of protons in the reaction mechanism as well as the likely decrease of the overpotential for 2,4-DCP oxidation. At higher pH (> 7.0), 2,4-DCP is ionized which led to the repulsion between negatively charged 2,4-DCP and sulfonate ions of Nafion present on the functionalized MWCNT surface that results in the absence of the oxidation peak in alkaline media. As the maximum current for oxidation of 2,4-DCP occurred in pH 6.0 phosphate buffer, therefore, the pH 6.0 was selected as the optimal pH for subsequent study.

On the basis of the results in Fig. 7b, a slope of 30 mV was obtained indicating the one proton two electron oxidation of 2,4-DCP. In the first step, 2,4-DCP is oxidized to phenoxy radical along with one electron and one proton transfer. Then, the phenoxy radical would lose one electron and oxidize to phenoxonium ion. The irreversible oxidation peak "O_1" for 2,4-DCP at ~+0.70 was derived from this stage. Analyzed from the previous literature on phenol oxidation (Chaplin, 2014; Grimshaw, 2000), it can be speculated that the oxidation of the hydroxyl group of 2,4-DCP occurs at more positive potential than the corresponding phenoxy radical, which oxidizes at less positive potential, therefore, eventually these two processes combine to give rise to a single two electron one proton transfer oxidation peak in 2,4-DCP. In other words, the phenoxy radical cannot be diamerized at MWCNT/Nafion/GCE and instead converted to catechol and hydroquinone in the presence of water.

The formation of these products was verified by analyzing multi-CVs of MWCNT/Nafion/GCE on the basis of the fact that the oxidation peak "O_1" is associated with the hydroxyl group of 2,4-DCP whereas the redox pairs (O_2/R_2 and O_3/R_1) represent the intermediate products of 2,4-DCP formed as a result of oxidation of phenoxy radicals. No oxidation or reduction peaks were found when potential scanned from −0.5 V to +0.5 V indicating that 2,4-DCP cannot be oxidized in this potential range. However, upon scanning the potential range from −0.5 V to +1.0 V an irreversible oxidation peak "O_1" at ~+0.70 V was due to the formation of phenoxy radical with the loss of one electron. The resulting phenoxy radicals were captured by the well-defined pores of MWCNT and oxidized at the catalytic active site in the vicinity to other offshoots such as catechol and hydroquinone. Being oxidized at considerably less positive potential, the hydroquinone and catechol therefore, immediately further oxidized to chlorinated benzoquinone. The formation of chlorinated benzoquinone from catechol and hydroquinone is a reversible process with two electrons and two protons transfer and this is the origin of a redox peak pairs of "O_2/R_2" and "O_3/R_1". As shown in Fig 3b (curves b), the reduction peaks "R_1" and "R_2" occurred at ~+0.23 V and ~+0.06 V on the reverse cathodic scan attributed to reduction of catechol and hydroquinone. Different from the first scan, in the second CV scan, two very weak oxidation peaks "O_2" and "O_3" appeared as a result of drop of oxidation peak "O_1". This behavior, the appearance of reduction and oxidation peaks ("R_1", R2, "O_2", and "O_3") at the expense of peak "O_1", clearly shows that the redox peak pairs (O_2/R_2 and O_3/R_1) are derived from the intermediate products of 2,4-DCP. On the subsequent cycles the oxidation peak "O_1" was recovered along with the growth in the peak currents of redox pairs (O_2/R_2 and O_3/R_1). However, after the fifth scan, the merge of the redox pairs was started and in tenth scan, they appeared almost as one pair of large peaks. The proposed mechanism based on above discussion is shown in Scheme 1.

3.7. Reproducibility, linear rang, and detection limit

The DPV analysis of MWCNT/Nafion/GCE at different times of day on different days showed better reproducibility and stability of the modified electrode. The oxidation peak current of 2,4-DCP retained over 95% of its initial current without any change in peak potential. However, after two weeks the

dramatic decrease in the oxidation peak was apparent. The relative standard deviation as a measure of the reliability of the electrode performance was well below 3%, which indicates its high reproducibility. The DPV curves of MWCNT/Nafion/GCE proportional to the different concentrations of 2,4-DCP and the corresponding calibration plot are shown in Fig. 8a and b, respectively. There is a well-behaved linear relationship between oxidation peak current and the concentrations of 2,4-DCP which covers the range of 1–150 μmol/L. The dynamic linear equation I (μA) = 0.0912 C (μmol/L) + 6.5818 with a correlation coefficient of 0.991 and a detection limit of 0.01 μmol/L [3(standard error in blank/slope)] was achieved using signal-to-noise ratio of 3, whereas standard error in blank was estimated by replicate measurements in 0.1 mol/L pH 6.0 phosphate buffer. The detection limit for determination of 2,4-DCP at MWCNT/Nafion/GCE is well matched with the maximum limit set by the European Union (0.5 μg/L) and U.S. EPA (1 μg/L) for eleven common phenols in drinking water (Igbinosa et al., 2013; Silva et al., 2009). Upon comparison the performance of the proposed method with other reported methods for the determination of 2,4-DCP, Table 1, it shows that the detection limit of MWCNT/Nafion/GCE is lower than the other electrochemical and optical methods. Moreover, the flow injection analysis with amperometric detection for 2,4-DCP using carbon nanotube has been proposed previously (Arribas et al., 2011) but presents some drawbacks that are similar to chromatographic methods, and due to complicated handling procedure the portability of the methods is not easily ensured. Therefore, with shorter analysis time and low detection limit, the proposed method is an excellent and simple alternative for the electrochemical determination of 2,4-DCP in water.

3.8. Interferences

Table 2 lists the tolerance level and % RSD of some of the substances that possibly disturb the determination of 2,4-DCP in water. The presence of chloro derivatives such as 2-chlorophenol (2-CP), 3-chlorophenol (3-CP), and 4-chlorophenol (4-CP) in the same test solution showed significant influence on the oxidation peak current and the oxidation peak potential of 2,4-DCP, because of the oxidation of the same hydroxyl group at or near the same oxidation potential of 2,4-DCP. However, at very low concentration no effects were observed. Fig. 9 shows the DPV curves of 2,4-DCP with different added concentrations of 3-CP. It was found that the oxidation peak of 2,4-DCP at $\sim+0.70$ V remained unaffected up to 10 μmol/L 3-CP however, above this a new peak appeared at $\sim+0.77$ V, identified as the oxidation peak of 3-CP, which on further increasing the concentration of 3-CP continues to increase. In other words, the increase in the oxidation peak current of 2,4-DCP in the presence of 20–100 μmol/L 3-CP means that the interference of 3-CP to 2,4-DCP. The nitrophenol derivatives and most of the other inorganic ions had an ignorable influence on the determination of 2,4-DCP.

3.9. Application tap water samples

The DPV detection of 2,4-DCP in tap water samples, under optimized conditions, showed no signal for any oxidation or reductions peaks, therefore, the standard addition method was adopted for the determination of 2,4-DCP. The results of different concentrations of 2,4-DCP detected 3 times by DPV method are shown in Table 3. It can be seen that the results obtained by DPV are in good agreement with the actual addition and the recovery is in the range of 99.0–102.5%. The less than 3% RSD and excellent recovery suggests that the proposed method is practical and reliable for determination of 2,4-DCP in real water samples.

4. Conclusion

A feasible electrochemical sensing platform using functionalized MWCNT modified on GCE, with superior electrocatalytic activity and better detection limit, for the determination of 2,4-DCP was developed. The fabrication MWCNT/Nafion/GCE is facile and rapid which reduces the analysis time. At MWCNT/Nafion/GCE, a remarkably sensitive and reproducible oxidation peak for 2,4-DCP, shifted toward less positive potential compared with bare GCE, was detected. The excellent analytical features of the proposed modified electrode are thus expected for its application in monitoring of 2,4-DCP and other phenols in real water samples.

Acknowledgments

We thankfully recognize the financial support from the Center of Excellence in Environmental Studies (CEES), King Abdulaziz University, and the Ministry of Higher Education (MOHE).

Appendix A. Supplementary material

Supplementary data associated with this article can be found, in the online version, at http://dx.doi.org/10.1016/j.arabjc.2015.08.032.

References

Amin, S., Soomro, M.T., Memon, N., Solangi, A.R., Sirajuddin, Qureshi, T., Behzad, A.R., 2014. Environ. Nanotechnol. Monit. Manage. 1–2, 8–13.

Arribas, A.S., Moreno, M., Bermejo, E., Pérez, J.A., Román, V., Zapardiel, A., Chicharro, M., 2011. Electroanalysis 23, 237–244.

Aslam, M., Ismail, I.M.I., Chandrasekaran, S., Hameed, A., 2014. J. Hazard. Mater. 276, 120–128.

Aslam, M., Soomro, M.T., Ismail, I.M.I., Salah, N., Waqar Ashraf, M., Qari, H.A., Hameed, A., 2015a. Arabian J. Chem. http://dx.doi.org/10.1016/j.arabjc.2015.05.001.

Aslam, M., Soomro, M.T., Ismail, I.M.I., Salah, N., Gondal, M.A., Hameed, A., 2015b. J. Environ. Chem. Eng. 3, 1901–1911.

Aslam, M., Qamar, M.T., Soomro, M.T., Ismail, I.M.I., Salah, N., Almeelbi, T., Gondal, M.A., Hameed, A., 2016. Appl. Catal. B 180, 391–402.

Barsan, M.M., Ghica, M.E., Brett, C.M.A., 2015. Anal. Chim. Acta 881, 1–23.

Bashami, R.M., Hameed, A., Aslam, M., Ismail, I.M.I., Soomro, M. T., 2015. Anal. Methods 7, 1794–1801.

Berhanu, D., Dybowska, A., Misra, S.K., Stanley, C.J., Ruenraroengsak, P., Boccaccini, A.R., Tetley, T.D., Luoma, S.N., Plant, J. A., Valsami-Jones, E., 2009. Environ. Health 8, S3.

Biniak, S., Pakuła, M., Świątkowski, A., Kuśmierek, K., Trykowski, G., 2015. Reac. Kinet. Mech. Cat. 114, 369–383.

Chaplin, B.P., 2014. Environ. Sci. Process. Impact. 16, 1182–1203.
Chen, M.L., Oh, W.C., 2011. Nanoscale Res. Lett. 6, 398–405.
Chen, A., Shah, B., 2013. Anal. Methods 5, 2158–2173.
Datsyuk, V., Kalyva, M., Papagelis, K., Parthenios, J., Tasis, D., Siokou, A., Kallitsis, I., Galiotis, C., 2008. Carbon 46, 833–840.
Ezerskis, Z., Jusys, Z., 2001. Pure Appl. Chem. 73, 1929–1940.
Ežerskis, Z., Jusys, Z., 2001. J. Appl. Electrochem. 31, 1117–1124.
Fan, C., Li, N., Cao, X., 2015a. Food Chem. 174, 446–451.
Fan, C., Li, N., Cao, X., 2015b. J. Sep. Sci. 38, 2109–2116.
Feng, Q.Z., Zhao, L.X., Yan, W., Lin, J.M., Zheng, Z.X., 2009. J. Hazard. Mater. 167, 282–288.
Feng, Q., Li, H., Zhang, Z., Lin, J.M., 2011. Analyst 136, 2156–2160.
Govindhan, M., Lafleur, T., Adhikari, B.R., Chen, A., 2015. Electroanalysis 27, 902–909.
Grassi, G., Scala, A., Piperno, A., Iannazzo, D., Lanza, M., Milone, C., Pistone, A., Galvagno, S., 2012. Chem. Commun. 48, 6836–6838.
Grimshaw, J., 2000. In Electrochemical Reactions and Mechanisms in Organic Chemistry. Elsevier Science, Amsterdam.
Gupta, V., Saleh, T., 2001. Syntheses of carbon nanotube-metal oxides composites; adsorption and photo-degradation. In: Bianco, Stefano (Ed.), Carbon Nanotubes – From Research to Applications. InTech.
Ho, T.T., Chen, C.Y., Li, Z.G., Yang, T.C., Lee, M.R., 2012. Anal. Chim. Acta 712, 72–77.
Igbinosa, E.O., Odjadjare, E.E., Chigor, V.N., Igbinosa, I.H., Emoghene, A.O., Ekhaise, F.O., Igiehon, N.O., Idemudia, O.G., 2013. Sci. World J. 2013, 460215.
Ijeri, V., Cappelletto, L., Bianco, S., Tortello, M., Spinelli, P., Tresso, E., 2010. J. Membr. Sci. 363, 265–270.
Jantra, J., Zilouei, H., Liu, J., Guieysse, B., Thavarungkul, P., Kanatharana, P., Mattiasson, B., 2005. Anal. Lett. 38, 1071–1083.
Kolliopoulos, A.V., Kampouris, D.K., Banks, C.E., 2015. Analyst 140, 3244–3250.
Lee, K., Lee, J.W., Kim, S.I., Ju, B.K., 2011. Carbon 49, 787–792.
Li, J., Zhao, X., Shi, Y., Cai, Y., Mou, S., Jiang, G., 2008a. J. Chromatogr. A 1180, 24–31.
Li, C., Thostenson, E.T., Chou, T.W., 2008b. Compos. Sci. Technol. 68, 1227–1249.
Li, Y., Jiao, Y., Guo, Y., Yang, Y., 2013. Anal. Methods 5, 5037–5043.
Lü, X., Wu, Z., Shen, J., Feng, J., Wang, Y., Song, Y., 2013. Int. J. Electrochem. Sci. 8, 2229–2237.
Lu, D., Feng, C., Wang, D., Lin, Y., Ip, H., She, J., Xu, Q., Wu, C., Wang, G., Zhou, Z., 2015. Anal. Bioanal. Chem. 407, 4131–4141.
Ozkan, D., Kerman, K., Meric, B., Kara, P., Demirkan, H., Polverejan, M., Pinnavaia, T.J., Ozsoz, M., 2002. Chem. Mater. 14, 1755–1761.
Ozsoz, M., Erdem, A., Ozkan, D., Kerman, K., Pinnavaia, T.J., 2003. Langmuir 19, 4728–4732.
Pirvu, C., Marcu, M., Banu, A., 2010. Rev. Chim. (Bucharest) 61, 585–589.
Pontié, M., Thouand, G., De|Nardi, F., Tapsoba, I., Lherbette, S., 2011. Electroanalysis 23, 1579–1584.
Safavi, A., Maleki, N., Tajabadi, F., 2014. Analyst 132, 54–58.
Saleh, T.A., 2013. The role of carbon nanotubes in enhancement of photocatalysis. In: Suzuki, Satoru (Ed.), Syntheses and Applications of Carbon Nanotubes and Their Composites. InTech.
Sherly, E.D., Vijaya, J.J., Selvam, N.C.S., Kennedy, L.J., 2014. Ceram. Int. 40, 5681–5691.
Shi, Q., Wang, H., Liu, S., Pang, L., Bian, Z., 2015. Electrochim. Acta 178, 92–100.
Silva, S., Alves, A., Santos, L., 2009. J. Chromatogr. Sci. 47, 103–109.
Stancu, M., Ruxanda, G., Ciuparu, D., Dinescu, A., 2011. Optoelectron. Adv. Mat. 5, 846–850.
Sun, D., Zhang, H., 2006. Water Res. 40, 3069–3074.
Tasic, T., Gupta, V.K., Antonijevic, M.M., 2014. Int. J. Electrochem. Sci. 9, 3473–3490.
Tong, Y., Li, D., Huang, J., Zhang, C., Li, K., Ding, L., 2013. Bull. Korean Chem. Soc. 34, 3307–3311.
Tonle, I., Ngameni, E., Tchieno, F.M., Walcarius, A., 2015. J. Solid State Electrochem. 19, 1949–1973.
Trojanowicz, M., 2006. TrAC Trend. Anal. Chem. 25, 480–489.
Ureta-Zañartu, M.S., Bustos, P., Diez, M.C., Mora, M.L., Gutiérrez, C., 2001. Electrochim. Acta 46, 2545–2551.
Ureta-Zañartu, M.S., Bustos, P., Berríos, C., Diez, M.C., Mora, M.L., Gutiérrez, C., 2002. Electrochim. Acta 47, 2399–2406.
Wang, J., Chatrathi, M.P., Tian, B., 2000. Anal. Chim. Acta 416, 9–14.
Wang, J., Deo, R.P., Musameh, M., 2003. Electroanalysis 15, 1830–1834.
Wei, X., Zhou, Z., Hao, T., Li, H., Xu, Y., Lu, K., Wu, Y., Dai, J., Pan, J., Yan, Y., 2015. Anal. Chim. Acta 870, 83–91.
Xu, Q., Li, X., Zhou, Y.-E., Wei, H., Hu, X.-Y., Wang, Y., Yang, Z., 2012. Anal. Methods 4, 3429–3435.
Yang, S., Yang, R., Li, G., Qu, L., Li, J., Yu, L., 2010. J. Electroanal. Chem. 639, 77–82.
Yang, Z.J., Huang, X.C., Li, J., Ren, Y.Y., Hu, X.Y., 2012. Adv. Mat. Res. 391–392, 1387.
Yu, P., Sun, Q., Li, J., Tan, Z., Yan, Y., Li, C., 2015. J. Environ. Chem. Eng. 3, 797–806.
Zhang, B., Xu, Y., Zheng, Y., Dai, L., Zhang, M., Yang, J., Chen, Y., Chen, X., Zhou, J., 2011. Nanoscale Res. Lett. 6, 431–440.
Zhang, J., Lei, J., Ju, H., Wang, C., 2013a. Anal. Chim. Acta 786, 16–21.
Zhang, Z., Zheng, J., Zhang, Y., Zhang, W., Li, L., Cao, Z., Wang, H., Li, C., Gao, Y., Liu, J., 2013b. Int. J. Electrochem. Sci. 8, 4183–4193.
Zheng, X., Lin, R., Zhou, X., Zhang, L., Lin, W., 2012. Anal. Methods 4, 482–487.